Transactions, SMiRT-25
Charlotte, NC, USA, August 4-9, 2019
Division V

TORSIONAL AND ROCKING RESPONSE OF A BASE ISOLATED NUCLEAR POWER PLANT

Satyam Kumar[1] and Manish Kumar[2]

[1]*PhD Student, Department of Civil Engineering, Indian Institute of Technology Bombay, India*
[2]*Assistant Professor, Department of Civil Engineering, Indian Institute of Technology Bombay, India*

ABSTRACT

The torsional and rocking responses of a seismically isolated nuclear power plant (NPP) is critical to the design of piping and auxiliary systems crossing through the isolation interface. The in-plan torsional response of the isolated superstructure depends on the eccentricity in the horizontal plane, ground motion characteristics, and properties of the isolation system. Torsional motion amplifies the horizontal response at the isolation interface. The rocking response of an isolated NPP depends on the height of the center of mass of the superstructure, axial stiffness of the isolators, ground motion characteristics, and the soil properties. The rocking motion amplifies the horizontal and vertical response at the isolation level and in the superstructure. The bearings along the periphery of the isolation interface are especially susceptible to buckling in compression and cavitation in tension due to the rocking motion of the superstructure.

This paper presents the torsional and the rocking response estimates of a base-isolated NPP subject to ground motion shaking at a location of high seismic hazard. Two model representations of a base-isolated NPP are created in OpenSees and LS-DYNA with isolation systems of different time-periods and strengths. The torsional and the rocking response of base-isolated NPPs are obtained subject to a series of ground motions scaled and spectrally matched to a specific hazard level. Superstructure with different in-plan eccentricities is analyzed to obtain the lower and upper bounds on the response. The effect of model parameters on the rotational and torsional response is also investigated. Amplification factors to account for the effect of torsional and rocking motions of the superstructure on the horizontal and vertical response of the isolation system are proposed.

INTRODUCTION

Seismic isolation is an earthquake resistant design technique that reduces the horizontal response of a structure to ground excitation by introducing horizontally flexible and vertically stiff layer between the superstructure and its substructure. Application of base isolation to a structure significantly increases its fundamental period of vibration compared to the corresponding fixed-base structure. Seismic isolation using low damping rubber (LDR) and lead-rubber (LR) bearings has shown to be a viable strategy to reduce the damaging effects of an earthquake (e.g., Kumar *et al.* (2014); Kumar *et al.* (2015a), Kumar *et al.* (2015b), Kumar *et al.* (2015d)). The past research has not investigated the in-plane rotation and vertical rocking response of the superstructure of a base-isolated NPP, which would be critical to the design of safety-related secondary components and equipment. In-plane torsional motion amplifies the resultant horizontal displacement of the bearings closer to the periphery of the isolation system. Rocking motion in the vertical plane of the structure amplifies the axial response in the peripheral isolators and might lead to buckling or cavitation in the LR bearings. This paper presents the torsional and rocking response estimates of NPPs seismically isolated using LR bearing subjected to a series of ground motions that are scaled and matched to a specific hazard level. A series of isolation systems of different time-periods (T) and strength to supported weight ratios (Q_d/W) are considered, and their influence on rocking and torsional response are studied. The effect of in-plan eccentricity on the torsional response is also investigated.

NPP MODEL

Two representations of the base isolated NPP, LMS model in OpenSees (McKenna *et al.*, 2006) and the FE model in LS-DYNA (LSTC, 2012), are shown in Figure 1 and Figure 2, respectively. The NPP is isolated using a basemat of dimension 100m×60m×2.5m. The total mass of the NPP, including the basemat, is approximately 151,000 tonnes.

The LMS model is recreated in OpenSees from EPRI (2007), which provides the equivalent nodal and element properties of the stick models created in SAP2000 (CSI, 2007). The three-dimensional model of NPP is simplified to three concentric lumped-mass stick models of the Coupled Auxiliary and Shield Building (ASB), Containment Internal Structure (CIS), and the Steel Containment Vessel (SCV). These three constitute approximately 59%, 38%, and 3% of the total mass of the NPP superstructure. The NPP is isolated through a common basemat slab on LR bearings, as shown in Figure 1. A symmetric layout of isolators is used underneath the basemat with the distance between the centers of adjacent bearings equal to 5 m, which requires a total of N_b = 273 isolators. Corner nodes are used as monitoring points to obtain the torsional and rocking response of the NPP.

The FE model of the representative NPP described in Orr (2003) was created in LS-DYNA (LSTC, 2012). This NPP consists of an Auxiliary Building (AB), a Concrete Containment Vessel (CCV), and a Containment Internal Structure (CIS), all sharing a common basemat. The CIS is joined only to the basemat, and the AB is joined to the CCV. The AB and CCV are modeled using shell elements, and the CIS and basemat are modeled using solid elements. Linear elastic properties for concrete and steel materials are assumed. The dimensions of the NPP are shown in Figure 2.

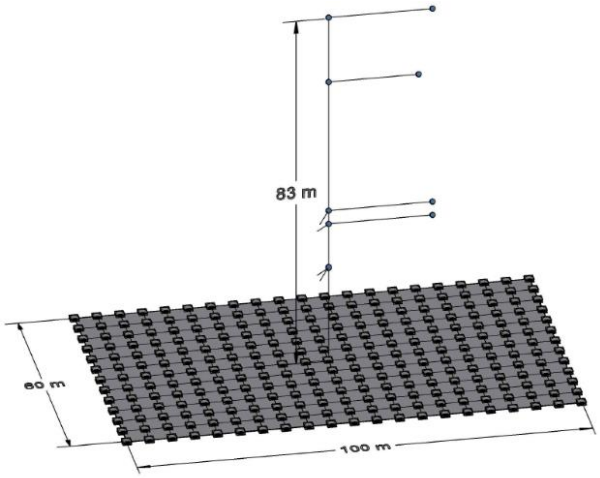

Figure 1: Lumped Mass Stick model of a base-isolated NPP in OpenSees (Kumar *et al.*, 2015d)

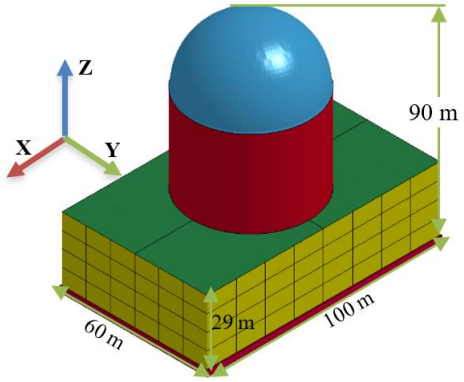

Figure 2. Finite element model of the reactor building (Kumar *et al.*, 2018)

The eccentricity between the center of mass of the superstructure and center of rigidity of the isolation system cannot always be avoided. The FE model in LS-DYNA is symmetric with zero eccentricity. However, the LMS model in OpenSees has small eccentricity due to the unsymmetrical layout of the superstructure. Additional LMS models with non-zero eccentricities are created in OpenSees to investigate the effect of eccentricity on the torsional response of the base-isolated NPP. All mass of the superstructure (e.g., ASB, CSI, SCV) is lumped to the rigid basemat of the LMS model in OpenSees at different locations to achieve the desired eccentricities along the two horizontal directions.

ISOLATION SYSTEM

The NPP superstructure is seismically isolated using a common basemat supported on 273 LR bearings. The layout of the isolation system for the LMS and the FE model are shown in Figure 3. The bearings are

spaced at an approximate center-to-center distance of 5m. Twelve LMS models are created in OpenSees with the following isolation systems: two isolation time period (T = 2,3 seconds) and six different strength to supported weight ratio (Q_d/W = 0.03, 0.06, 0.09, 0.12, 0.15, and 0.18). Two FE model is created in LS-DYNA of the time period, T =2, 3 seconds, and strength to weight ratio, Q_d/W = 0.12. The models are denoted by *TxQy*, where *x* identifies the value of T and *y* identifies the percentage of Q_d/W.

The LR bearing in OpenSees is modeled using *LeadRubberX*. The detailed information on the *LeadRubberX* is presented in Kumar *et al.* (2014). For this study, a simplified numerical model of the LR bearing is considered without including the advance behavior options available in *LeadRubberX*.

The lead rubber bearing in LS-DYNA is modeled using the discrete isolator element (*MAT SEISMIC_ISOLATOR). It considers the linear elastic behavior in the axial direction with the same stiffness in compression and tension. The coupled bi-directional hysteretic behavior in the horizontal direction is modeled using the formulation proposed by Park *et al.* (1986) and extended for seismic isolators by Nagarajaiah *et al.* (1989).

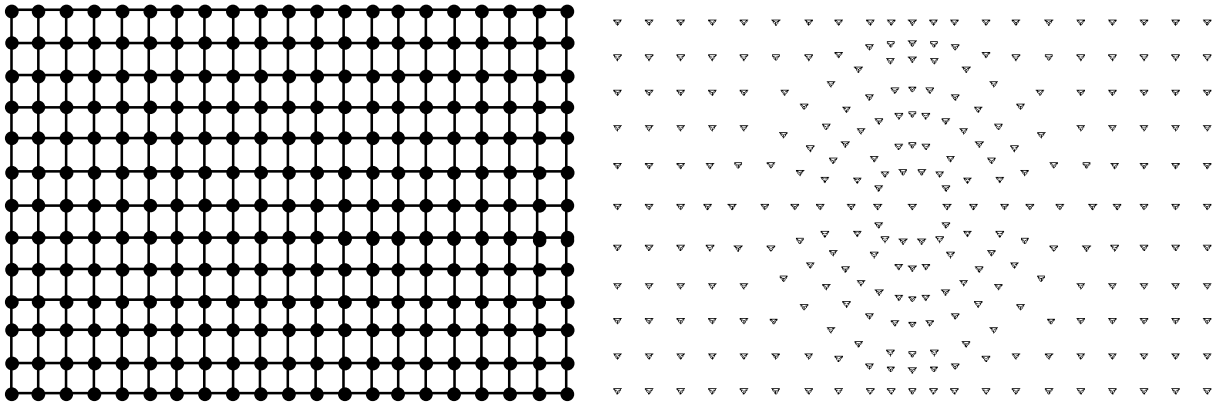

a) Lumped mass stick model in OpenSees b) Finite element model in LS-DYNA

Figure 3: Layout of the isolators in the isolation system

The material and geometric properties of the isolators for each isolation system are calculated from isolation time-period (T) and strength to supported weight ratio (Q_d/W). The detailed procedure is described in Kumar *et al.* (2015d). The summary of the geometrical and mechanical properties of the isolators for different isolation system designs are presented in Table 1 and Table 2.

Table 1. Geometric and mechanical properties of the LR bearing for isolation period of 2.0 sec

Property	Notation	*T2Q3*	*T2Q6*	*T2Q9*	*T2Q12*	*T2Q15*	*T2Q18*
Single rubber layer thickness (mm)	t_r	10	10	10	10	10	10
Number of rubber layer	n	27	27	27	27	27	27
Steel shim thickness (mm)	t_s	4.76	4.76	4.76	4.76	4.76	4.76
Outer diameter (mm)	D_o	1500	1514	1522	1530	1538	1546
Lead core diameter (mm)	D_i	156	222	272	314	350	384
Rubber cover thickness (mm)	t_c	25.4	25.4	25.4	25.4	25.4	25.4
Shear modulus (MPa)	G	0.8	0.8	0.8	0.8	0.8	0.8
Bulk modulus of rubber (MPa)	K_{bulk}	2000	2000	2000	2000	2000	2000
Yield stress of lead (MPa)	σ_L	8.5	8.5	8.5	8.5	8.5	8.5
Yield displacement (mm)	U_y	21	21	21	21	21	21
Static bearing pressure (MPa)	P_{static}	3	3	3	3	3	3
Post elastic shear stiffness (MN/m)	K_H	5.50	5.50	5.50	5.50	5.50	5.50
Vertical stiffness (MN/m)	K_{vo}	7851	7799	7760	7728	7698	7671

Table 2. Geometric and mechanical properties of the lead rubber bearing for isolation period of 3.0 sec

Property	Notation	*T3Q3*	*T3Q6*	*T3Q9*	*T3Q12*	*T3Q15*	*T3Q18*
Single rubber layer thickness (mm)	t_r	10	10	10	10	10	10
Number of rubber layer	n	60	60	60	60	60	60
Steel shim thickness (mm)	t_s	4.76	4.76	4.76	4.76	4.76	4.76
Outer diameter (mm)	D_o	1500	1514	1522	1531	1538	1546
Lead core diameter (mm)	D_i	156	222	272	314	351	384
Rubber cover thickness (mm)	t_c	25.4	25.4	25.4	25.4	25.4	25.4
Shear modulus (MPa)	G	0.8	0.8	0.8	0.8	0.8	0.8
Bulk modulus of rubber (MPa)	K_{bulk}	2000	2000	2000	2000	2000	2000
Yield stress of lead (MPa)	σ_L	8.5	8.5	8.5	8.5	8.5	8.5
Yield displacement (mm)	U_y	21	21	21	21	21	21
Static bearing pressure (MPa)	P_{static}	3	3	3	3	3	3
Post elastic shear stiffness (MN/m)	K_H	2.44	2.44	2.44	2.44	2.44	2.44
Vertical stiffness (MN/m)	K_{vo}	3489	3466	3449	3434	3421	3409

MODAL ANALYSIS

Theoretical values of the time-periods of the base-isolated NPP are calculated using a simplified model of the base-isolated NPP shown in Figure 4. The geometric properties of the LMS model, presented in Table 3, were used to calculate the theoretical time-periods of the simplified NPP model.

Table 3. Location of the center of masses of the components of the LMS model

			Mass (ton)	X (m)	Y (m)	Z (m)
Superstructure (M_S)	ASB/AB	LMS	63743	-0.45	28.7	0.90
		FE	61917	0.00	45.7	0.00
	CIS	LMS	41009	-0.33	9.9	0.33
		FE	3289	0.00	17.0	0.00
	SCV/CCV	LMS	3734	0.00	41.3	0.00
		FE	34846	0.00	45.7	0.00
	Total	LMS	108486	-0.39	22.0	0.65
		FE	100052	0.00	27.0	0.00
Basemat (M_b)		LMS	42450	0.00	0.4	0.00
		FE	51500	0.00	2.1	0.00
Total ($M_S + M_b$)		LMS	150936	-0.28	15.8	0.47
		FE	151552	0.00	18.4	0.00

A simplified schematic representation of the base-isolated NPP is provided in Figure 4. The theoretical values of the frequencies of the simplified model are calculated using the following expressions:

$$f_{\text{Horizontal}} = \frac{1}{2\pi}\sqrt{\frac{\sum_{i=1}^{N_b} K_H}{M_b + M_s}} \qquad f_{Axial} = \frac{1}{2\pi}\sqrt{\frac{\sum_{i=1}^{N_b} K_V}{M_b + M_s}}$$

$$f_{Torsional} = \frac{1}{2\pi}\sqrt{\frac{\sum_{i=1}^{N_b} K_H X_i^2 + K_H Y_i^2}{(M_b + M_s)\mathrm{r}_T^2}} \qquad f_{Rocking} = \frac{1}{2\pi}\sqrt{\frac{\sum_{i=1}^{N_b} K_V X_i^2}{(M_b + M_s)\mathrm{r}_R^2}}$$

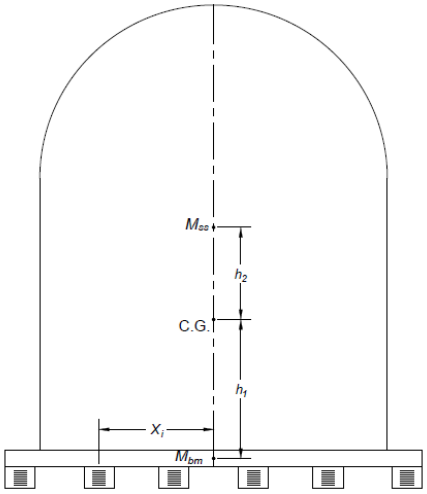

Figure 4. A simplified model of the base isolated NPP

where r_R and r_T represents the radius of gyration about the rocking axis and vertical axis respectively. Other parameters are shown in Figure 4.

Modal analysis of the numerical models of the base-isolated NPPs was performed in OpenSees and LS-DYNA, and the results are presented in Table 4. A good comparison between the modal time-periods is obtained in all directions. Two additional LMS models are created by removing all superstructure components (e.g., ASB, CIS, SCV) and lumping it at specific locations at the basemat level to achieve 0% and 5% eccentricities. The torsional period is reduced significantly to 1.1 sec. This model is further used to estimate the in-plan torsional response of base-isolated NPPs at different values of eccentricities.

Table 4. Modal time-periods of the numerical models in OpenSees (LMS) and LS-DYNA

Mode		Theoretical	OpenSees			LS-DYNA
			LMS (e= 0%)	LMS (e=5%)	LMS	
1	Horizontal 1	2.001	2.022	2.059	2.047	2.010
2	Horizontal 2	2.001	2.022	2.022	2.046	2.013
3	Torsion	1.892	1.091	1.100	1.464	2.024
4	Rocking 1	0.049	n.a.	n.a.	-	-
5	Rocking 2	0.051	n.a.	n.a.	-	-
6	Axial	0.053	n.a.	n.a.	-	-

n.a.= not applicable for the given model

DAMPING

Two types of damping definitions are used to represent the energy dissipation characteristics of a structure, namely, hysteretic damping and viscous damping. The hysteretic energy dissipation in an LR bearing is provided by lead-core and modeled explicitly using a hysteresis model. The contribution of rubber to energy dissipation in the lateral and axial direction is modeled using equivalent viscous damping. The contribution of lead core to the axial energy dissipation is neglected.

For the LMS model in OpenSees, the isolation system was assigned a supplementary 2% damping (in addition to hysteretic) based on the horizontal isolation frequency (e.g., 0.5 *Hz*) and the vertical frequency (e.g., 18.7 *Hz*). The elastic superstructure was assigned a Rayleigh damping of 4% based on the first horizontal mode of ASB (2.77 Hz) and the second horizontal mode (12.52 *Hz*) of the CIS.

For the FE model in LS-DYNA, the superstructure was assigned mass damping of 4% based on its first horizontal frequency and damping of 4% using a stiffness damping formulation defined in LS-DYNA that uniformly damps all the high-frequency modes (LSTC, 2016).

SEISMIC HAZARD

A uniform hazard response spectra (UHRS) was obtained corresponding to a return period of 10,000 years and 5% damping for the Diablo Canyon Nuclear Power Station. It is a site of high seismic hazard and houses two nuclear reactors. Thirty sets of the ground motions were selected and scaled to match the UHRS spectrum. Figure 5 illustrates that the average response spectra of the selected ground motions matching with the target response spectra. NIST (2011) provides a detailed procedure of selection and the matching of ground motion. Complete details on the ground motions are presented in Kumar *et al.* (2015e). Response history was performed using these 30 ground motions for different base-isolated NPP models in OpenSees and LS-DYNA. The analysis results are presented in the following section.

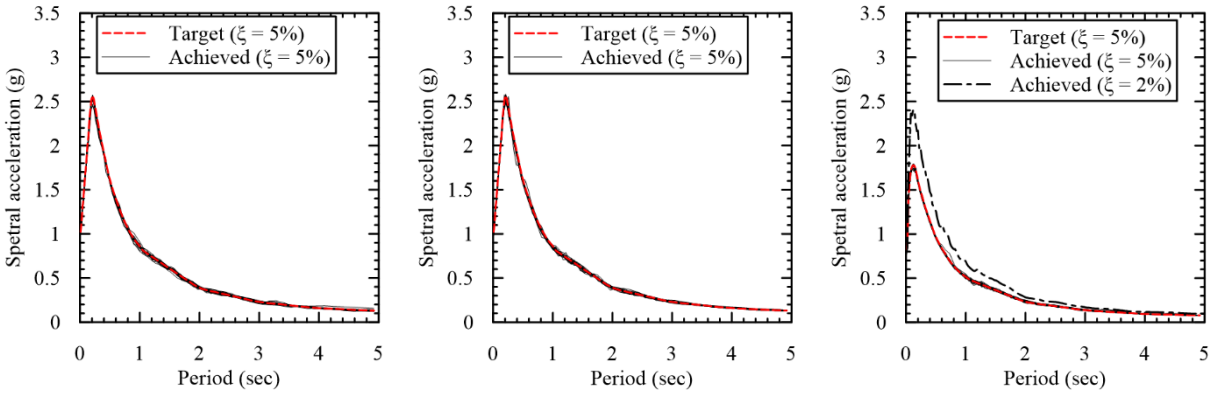

a) X-direction (Translational) b) Y-direction (Translational) c) Z-direction (vertical)

Figure 5. Acceleration response spectra of ground motions

RESULTS

The peak horizontal response of the base-isolated NPPs at the center of the basemat is presented in Table 5. The displacement values at the basemat center serve as a reference to evaluate the amplification at off-center locations due to the torsional and rocking motions. An in-plane torsion angle of 0.01 degrees corresponds to 10 mm of horizontal displacement over the basemat length of 100 m. A rocking angle of 0.0005 degrees corresponds to 0.5 mm of vertical displacement over the basemat length of 100 m. The torsional and rocking responses of the base-isolated NPPs are presented in Table 6 through Table 9. Mean, and percentile values are calculated by assuming that the peak responses for each of the 30 ground motion set are lognormally distributed. Variation of the torsional and rocking response with a change in characteristics strength to weight ratio of the isolation system of the NPP are presented in Figure 6 and Figure 7, respectively. The in-plane torsional displacement decreases with the increase in the strength and the time-period of the isolation system. Its contribution to the resultant horizontal displacement at the corners of the isolated basemat is typically within 10% for the LMS model due to very small eccentricity. The symmetric FE models have negligible torsional rotation. The mean rocking response of the FE model in LS-DYNA is larger than the LMS model due to the higher location of the center of mass in the FE model, as reported in Table 3. The rocking response might contribute to an additional axial displacement of 1 mm, which might increase the probability of cavitation and buckling in the bearings close to the periphery of the isolation system. The estimated cavitation and buckling displacement of bearings are 0.57 mm and 19 mm for the T2Q12 isolation system.

Table 5. Peak horizontal displacement at the center of the isolated basemat (30 ground motions)

Model	LMS model in OpenSees					FE model in LS-DYNA				
	Mean	50th	90th	99th	σ	Mean	50th	90th	99th	σ
T2Q12	209	206	261	317	180	205	201	263	327	210
T3Q12	226	222	288	356	200	215	210	278	348	220

Table 6. Peak torsional response of the LMS model in OpenSees (30 ground motions)

Model	Mean		50th		90th		99th		σ
	Angle (degrees)	Disp. (mm)	Angle (degrees)	Disp. (mm)	Angle (degrees)	Disp. (mm)	Angle (degrees)	Disp. (mm)	
T2Q3	0.0140	14.3	0.0135	13.8	0.0194	20.0	0.0261	26.5	0.28
T2Q6	0.0105	10.6	0.0100	10.2	0.0146	14.9	0.0199	20.3	0.30
T2Q9	0.0084	8.6	0.0080	8.2	0.0120	12.2	0.0167	17.0	0.32
T2Q12	0.0072	7.4	0.0069	7.0	0.0104	10.6	0.0146	14.8	0.32
T2Q15	0.0064	6.5	0.0061	6.3	0.0091	9.3	0.0127	12.9	0.31
T2Q18	0.0059	6.0	0.0056	5.7	0.0084	8.5	0.0116	11.8	0.31
T3Q3	0.0119	12.2	0.0116	11.8	0.0163	16.6	0.0215	21.8	0.27
T3Q6	0.0092	9.4	0.0089	9.1	0.0123	12.5	0.0159	16.1	0.25
T3Q9	0.0077	7.8	0.0075	7.6	0.0102	10.4	0.0132	13.4	0.24
T3Q12	0.0070	7.1	0.0068	6.9	0.0092	9.4	0.0118	12.0	0.24
T3Q15	0.0061	6.2	0.0058	5.9	0.0090	9.1	0.0129	13.1	0.34
T3Q18	0.0060	6.1	0.0058	5.9	0.0082	8.3	0.0109	11.1	0.28

Table 7. Peak torsional response of the FE model in LS-DYNA (30 ground motions)

Model	Mean		50th		90th		99th		σ
	Angle (degrees)	Disp. (mm)	Angle (degrees)	Disp. (mm)	Angle (degrees)	Disp. (mm)	Angle (degrees)	Disp. (mm)	
T2Q12	0.0020	2.0	0.0020	2.1	0.0024	2.5	0.0028	2.9	0.15
T3Q12	0.0021	2.2	0.0021	2.2	0.0026	2.7	0.0032	3.3	0.19

Table 8. Peak rocking response LMS model in OpenSees (30 ground motions)

Model	Mean		50th		90th		99th		σ
	Angle (degrees)	Disp. (mm)	Angle (degrees)	Disp. (mm)	Angle (degrees)	Disp. (mm)	Angle (degrees)	Disp. (mm)	
*T2Q*3	0.0005	0.29	0.0005	0.28	0.0006	0.34	0.0007	0.39	0.13
*T2Q*6	0.0005	0.28	0.0005	0.28	0.0006	0.34	0.0008	0.39	0.14
*T2Q*9	0.0006	0.29	0.0006	0.29	0.0007	0.35	0.0008	0.41	0.14
*T2Q*12	0.0006	0.32	0.0006	0.32	0.0007	0.38	0.0008	0.43	0.13
*T2Q*15	0.0007	0.35	0.0007	0.35	0.0008	0.41	0.0009	0.47	0.13
*T2Q*18	0.0008	0.40	0.0008	0.40	0.0009	0.46	0.0010	0.53	0.13
*T3Q*3	0.0007	0.35	0.0007	0.35	0.0008	0.41	0.0009	0.47	0.13
*T3Q*6	0.0007	0.39	0.0007	0.39	0.0009	0.47	0.0010	0.55	0.15
*T3Q*9	0.0009	0.47	0.0009	0.46	0.0011	0.56	0.0013	0.66	0.15
*T3Q*12	0.0011	0.56	0.0011	0.55	0.0013	0.67	0.0015	0.79	0.15
*T3Q*15	0.0013	0.68	0.0013	0.67	0.0015	0.80	0.0018	0.93	0.14
*T3Q*18	0.0015	0.81	0.0015	0.80	0.0018	0.95	0.0021	1.10	0.14

Table 9. Peak rocking response of the FE model in LS-DYNA (30 ground motions)

Model	Mean		50th		90th		99th		σ
	Angle (degrees)	Disp. (mm)	Angle (degrees)	Disp. (mm)	Angle (degrees)	Disp. (mm)	Angle (degrees)	Disp. (mm)	
T2Q12	0.0008	0.4	0.0006	0.3	0.0020	1.1	0.0051	2.7	0.90
T3Q12	0.0016	0.8	0.0013	0.7	0.0044	2.3	0.0119	6.2	0.95

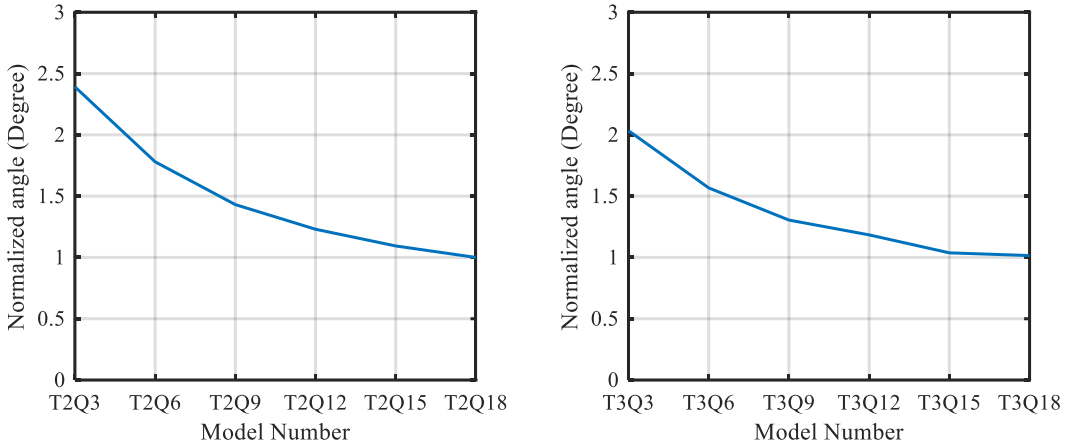

a) Isolator period = 2 seconds b) Isolator period = 3seconds

Figure 6. The normalized mean in-plan torsion of the isolated NPP models in OpenSees

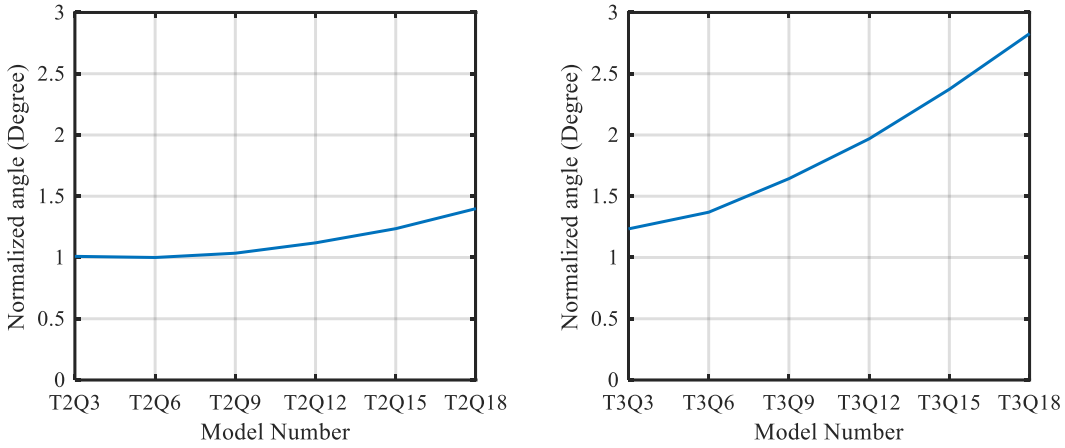

a) Isolator period = 2 seconds b) Isolator period = 3 seconds

Figure 7. The normalized mean rocking angle of the isolated NPP models in OpenSees

Additional modified LMS models were created by removing all superstructure components (e.g., ASB, CIS, SCV) and lumping it at the basemat level at different locations to achieve desired eccentricities in the two horizontal directions. Response history analysis is performed for these LMS models in OpenSees, and the displacements at the center and corners of the basemat are presented in Table 10 and Table 11, respectively. The torsional response is presented in Table 12.

Table 10. Peak horizontal displacement (mm) at the basemat center of the modified LMS model (T2Q12, 30 ground motions)

Eccentricity		Mean	50th	90th	99th	σ
e_x	e_y					
0%	0%	250	246	310	374	180
5%	5%	246	242	307	373	180
10%	10%	238	234	301	371	200
15%	15%	230	225	296	372	220
20%	20%	224	219	291	367	220

Table 11. Peak horizontal displacement (mm) at the basemat corner of the modified LMS model (T2Q12, 30 ground motions)

Eccentricity		Mean	50th	90th	99th	σ
e_x	e_y					
0%	0%	250	246	310	374	180
5%	5%	294	290	366	443	180
10%	10%	335	329	425	523	200
15%	15%	359	351	464	583	220
20%	20%	366	357	480	610	230

Table 12. In-plan rotation (torsion) in degrees of the isolated basemat (T2Q12, 30 ground motions)

Eccentricity		Mean		50th		90th		99th		σ
e_x	e_y	Angle	Disp. (mm)	Angle	Disp. (mm)	Angle	Disp. (mm)	Angle	Disp. (mm)	
0.28% (LMS)	1.55% (LMS)	0.007	7	0.007	7	0.010	10	0.015	15	0.32
0%	0%	0.000	0	0.000	0	0.000	0	0.001	0	0.92
5%	5%	0.092	93	0.088	90	0.127	129	0.171	174	0.28
10%	10%	0.155	157	0.149	152	0.215	218	0.289	294	0.30
15%	15%	0.193	196	0.186	189	0.267	271	0.358	364	0.28
20%	20%	0.220	224	0.212	215	0.303	309	0.406	413	0.28

For a plan basemat dimensions of 100m×60m (diagonal length=116.6m), an eccentricity of 5% result an additional displacement of 93.6 mm (0.092× (π/180) × 116.6/2 m). The eccentricity results in significant amplification of the horizontal displacement at the corners of the basemat while the horizontal displacement decreases at the center of the basemat with the increase in the eccentricity. The in-plane torsional displacement contributes 31.6% of the total resultant horizontal displacement at the corner of the basemat for the 5% eccentricity. This also emphasizes the importance of considering a three-dimensional representation of the base-isolated NPPs for response history analysis to accurately estimate the horizontal displacement of the isolators.

SUMMARY AND CONCLUSION

The torsional and rotational response of base-isolated NPPs were obtained using two representations of a base-isolated NPP, a lumped mass stick model, and a detailed FE model, in OpenSees and LS-DYNA respectively. Several isolation systems of the different time period and characteristics strength to weight ratio were analyzed subject to an earthquake shaking at the location of high seismic hazard. The effect of in-plan eccentricities on the torsional response was also investigated.

The key conclusion of this study are:

1. The rocking frequency of a base isolated NPP is typically much greater than the horizontal and the in-plan torsional frequencies.
2. The torsional response of the base isolated NPP decreases with the increase in the isolation time-period and the characteristics strength to supported weight ratio.
3. The rocking response of the base isolated NPP increases with the increase in the isolation time-period and the characteristics strength to supported weight ratio.
4. Increase in eccentricity from 5 % to 20% amplifies the mean in-plane torsional displacement by two and half times of the base isolated NPP.
5. The in-plan torsional response of a base-isolated NPP with eccentricity 5% can contribute 31.6% of the resultant horizontal response at the corners of the isolated basemat.

REFERENCES

Computer & Structures Inc. (CSI) (2007). "SAP2000 user's manual–version 11.0." Berkeley, CA.

Electric Power Research Institute (EPRI). (2007). "Program on technology innovation: validation of CLASSI and SASSI codes to treat seismic wave incoherence in soil-structure interaction (SSI) analysis of nuclear power plant structures." *EPRI Technical Report 1015111*, Palo Alto, CA.

Kammerer, A. M., Whittaker, A. S., and Constantinou, M. C. (2018). "Technical considerations for seismic isolation of nuclear facilities." NUREG/CR-7253, United States Nuclear Regulatory Commission, Washington, DC.

Kumar, M., Whittaker, A., and Constantinou, M. (2014). "An advanced numerical model of elastomeric seismic isolation bearings." *Earthquake Engineering and Structural Dynamics*, 43(13), 1955-1974.

Kumar, M., Whittaker, A., and Constantinou, M. (2015a). "Experimental investigation of cavitation in elastomeric seismic isolation bearings." *Engineering Structures*, 101, 290-305.

Kumar, M., Whittaker, A., and Constantinou, M. (2015b). "Response of base-isolated nuclear structures to extreme earthquake shaking." *Nuclear Engineering and Design*, 295, 860–874.

Kumar, M., Whittaker, A., and Constantinou, M. (2015c). "Characterizing friction in sliding isolation bearings." *Earthquake Engineering & Structural Dynamics*, 44(9), 1409-1425.

Kumar, M., Whittaker, A. S., and Constantinou, M. C. (2015d). "Seismic isolation of nuclear power plants using elastomeric bearings." Technical Report MCEER-15-0008, University at Buffalo, State University of New York, Buffalo, NY.

Kumar, M., Whittaker, A. S., and Constantinou, M. C. (2015e). "Seismic isolation of nuclear power plants using sliding bearings." Technical Report MCEER-15-0006, University at Buffalo, State University of New York, Buffalo, NY.

Kumar, M., and Whittaker, A. (2018). "Response of systems and components in a base-isolated nuclear power plant building impacted by a large commercial aircraft." *Journal of Structural Engineering*, 144(9).

Livermore Software Technology Corporation (LSTC) (2012). Computer Program LS-DYNA, Livermore, CA.

McKenna, F., Fenves, G., and Scott, M. (2006). Computer Program OpenSees: Open System for Earthquake Engineering Simulation, Pacific Earthquake Engineering Research Center, University of California, Berkeley, CA,(http://opensees.berkeley.edu).

Nagarajaiah, S., Reinhorn, A. M., and Constantinou, M. C. (1989). "Nonlinear dynamic analysis of three-dimensional base-isolated structures (3D-BASIS)." Technical Report NCEER-89-0019, University at Buffalo, State University of New York, Buffalo, NY.

National Institute of Standards and Technology (NIST). (2011). "Selection and scaling earthquake ground motions for performing response-history analyses." *Technical Report NIST GCR 11-917-15*, Gaithersburg, MD.

Park, Y. J., Wen, Y. K., and Ang, A. H. S. (1986). "Random vibration of hysteretic systems under bi-directional ground motions." *Earthquake Engineering and Structural Dynamics*, 14(4), 543-557.